



Prediction of Flyrocks, Airblasts and Ground Vibrations Using Neural Computing and Applications at ZCDC Mine

Charles Chewu¹, Tonderai Chikwere¹, Desire Runganga¹, Elia Chipfupi*¹, and Tatenda Nyamagudza¹

¹ Mining Engineering Department, Manicaland State University of Applied Sciences (M.S.U.A.S.), Mutare, Zimbabwe.

KEYWORDS

*Flyrock
Airblast
Multivariate Regression
Bayesian Regularisation*

ARTICLE HISTORY

*Received 30 January 2023
Received in revised form
7 June 2023
Accepted 30 August 2023
Available online 11 September
2023*

ABSTRACT

When an explosive detonates in a blasthole, approximately 20 to 30% of the energy is only utilized for fragmenting the rock mass whilst the bulk of the energy is lost in the form of ground vibrations, flyrocks and airblasts. Employees' residences, mine offices, processing plants and engineering workshops built close to the mining area and are in danger of being damaged by blast induced hazards. In addition, due to flyrocks there was a high level of ore losses, ore dilution, equipment damages, mine roads and powerlines. To assess and reduce these negative impacts, monitoring of flyrocks, ground vibrations and airblast was carried out and generate a prediction model. A three-layer, feed-forward back-propagation of a 9-10-3 network architecture was trained, validated, and tested using the Bayesian regularization algorithm. A total of 100 monitored blast records obtained from the mine were used as input parameters for the ANN prediction model. Subsequently a Multivariate Regression analysis prediction model was run and used to compare with the results obtained from ANN model. Based on the study's findings, an ANN model proved to be the best for field predictions. To determine the relative impact of each input parameter on flyrocks, ground vibration, and Airblast, a sensitivity analysis was also carried out and lastly blast optimization which managed to reduce blast induced impacts by over 30%.

© 2023 The Authors. Published by Penteract Technology.

This is an open access article under the CC BY-NC 4.0 license (<https://creativecommons.org/licenses/by-nc/4.0/>).

1. INTRODUCTION

The depth of the pits at Zimbabwe Consolidated Diamond Company (ZCDC) is now approaching 45 m below the ground level developing into the Ushonje mountain range, so due to the increase in the depth of the pit, a great danger of highwall collapse is keeping on and on increasing and hence a need to come up with measures to reduce blast induced ground vibration and ensure stability of the highwalls. There are some ore losses and ore contamination caused by flyrocks which resultantly causes a decline in overall mineral recovery per blast and some unnecessary expenses in the processing plants. There are some possible disturbances of the stability of slimes dams, employees' residences and mine offices due to blast induced ground vibration. Hence the need to have an understanding of the blasting system in-order to mitigate these detrimental effects.

Blasting process or simply detonation of explosives involves two energy forms being released which are, gas energy

and shock energy. The detonating energy used in blasting is generated from chemical energy stored in the explosives which results in large gaseous volumes that creates stresses on the blast hole. This results in strain energy created from strain waves on the particles surrounding the rock, this strain energy is responsible for breaking the rock into smaller pieces or what is known as muck pile [1].

Using good blast designs, the explosive energy can perform mostly fragmentation of rock mass without damage to the environment, high walls and mine structures. The major purpose of blasting in mining is to extract a high valued ore and get profits out of it. But this high valued ore is buried under large volumes of waste which requires much blasting to expose it. This blasting results in some adverse effects to the environment, mine, properties as well as peoples which includes; ground vibration, fly rocks, air blasts and noise [2].

It is also crucial to note that upon detonation of an explosive charge, approximately 20-30% of the energy is only

*Corresponding author:

E-mail address: Elia Chipfupi <echipfupi@gmail.com>.

<https://doi.org/10.56532/mjsat.v3i3.135>

2785-8901/ © 2023 The Authors. Published by Penteract Technology.

This is an open access article under the CC BY-NC 4.0 license (<https://creativecommons.org/licenses/by-nc/4.0/>).

utilized in fragmenting the rock and a portion of the energy is lost in form of ground vibrations, air blasts, noise and fly-rocks. The negative effects of ground vibrations, fly rocks and air blasts produced due to blasting affect both the structures around the blast site as well as the structures existing in the closed vicinity, peoples and animals. Although these negative cannot be totally done away with, there a number of techniques which have been devised to alleviate them [3].

Many techniques have been developed which try to model blasting system behavior, this includes Genetic Algorithms, Maximum likelihood classification, Artificial Neural Networks, Technique for Order Preference Similarity to Ideal Solution (TOPSIS) and many others. In this paper Artificial Neural Networks and Multivariate Analysis, which are amongst the most widely used techniques, have been explored and analysed in-order to model and predict the blasting system behavior [4][5].

This paper has been arranged in the following manner. Section 2 outlines the literature review of the project and discusses blasting parameters such as fly rocks, blast induced ground vibration, air blast and Artificial Neural Networks. Section 3 describes the project methodology. Section 4 focuses on results and their analysis. Section 5 concludes the paper.

2. LITERATURE REVIEW

The scope of this paper is limited to the study and control of fly rocks, air blast and ground vibration in a blasting scenario.

2.1 Fly Rocks

In a controlled explosion, flyrock is the rock that is expelled from the blast site during a mining operation. It particularly refers to the rock that flies beyond the blast site potentially causing property damages, injuries to people, and potentially mixing waste with ore. Flyrocks can vary in mass and coarse size. Fly rocks are caused mainly by poor stemming and poor or faulty blast designs [6].

An investigation was carried on generated flyrocks from rock blasting in surface mines demonstrated that injuries caused by flyrocks and poor blasting practices was amounting to 68% of blast injuries in metalliferous and non-metalliferous mines during the period 1978 to 2002. Emphasis was given on the measures to reduce blast induced fly rock incidents and accident by exercising proper blasting techniques. Uses projectile motion equation to come up with a prediction model to find out flyrock initial velocity, distance travelled by projected rock particles and shape of the rock fragments. It was established that, flyrocks can be generated by a mismatch of explosive energy generated with the rock strength. It was also established that the higher the explosive energy generated the higher the pressure gases emanating from blast holes in the weakest zone direction which causes excessive flyrocks throw [7].

The prediction of blast induced flyrocks using neural networks established that specified blast design such as improper drilling, burden, inappropriate delay timing, inadequate stemming length, very high explosive concentration, their sequence, loose rocks on the top of the bench due to poor previous blasts and back breaks are the major causes of flyrocks. It was further established that blast design parameters such as rock quality designation (RQD) and uniaxial

compressive strength (UCS) may be used as significant input parameters in artificial neural network (ANN) and multivariate linear regression analysis (MVRA) models of predicting flyrock distances [3][7].

2.2 Blast Induced Ground Vibrations

One of the negative impacts of blasting is ground vibration. Blast induced ground vibrations are always associated with waves of elastic in nature propagating through the ground which triggers particle motion. Blast induced ground vibration cause very high attenuation of the ground bearing strata which resultantly weakens high walls and cause high wall collapse weakens and causes cracks to mine office buildings, weakens the slimes dams and disturbs the straightness of the conveyor belts in the processing plants which ardently causes fast wear and tear of conveyors and rollers [8]. High Ground vibration is caused due to too much explosive. The higher the quantity of explosive that is being detonated the higher the quantity of energy that is being released [9].

Monitoring of ground vibration is very essential due to the follow reasons:

1. To ensure that vibration levels do not cause damage to neighboring properties
2. To prevent annoyance or nuisance to others by maintaining the lowest possible levels.
3. To identify measures that reduce the hazardous effects of vibration
4. To ensure regulatory compliance that is to make sure that the vibration produced is within the standard permissible limits.

Blasting vibration analysis is a simulation that models the blasting effects; therefore, analysis is needed to determine the level of vibration generated by the blasting activity and then formulate prediction models to help in coming up with measures to reduce the impact [10].

Ground vibrations are associated with the different types of elastic waves propagating through the ground which triggers particle motion. Stress waves are the waves which are generated because of the blasting in mines either open cast or underground mines. Stress waves propagates within the blasted material and the surface as well. Based on the characteristics of propagation and displacement basically in solid and the outer surface stress waves are divided into two groups which are body waves and surface waves. Body waves are generated when explosive inside holes is detonated using detonators and other means. Surface waves are generated when body waves are interacted on a free surface or in discontinuities in the rock mass. Furthermore, body waves are further divided into S-wave and P-wave and then surface waves are then sub divided into releigh wave, love wave and stonely wave [11].

The ground vibration is usually measured in terms of Peak Particle Velocity (PPV). The PPV is known as the maximum velocity particles travel resulting from the ground vibrations and it is measured in mm/s. Usually, blasting operations are performed at sites close to inhabited places or factory premises, where induced ground vibrations by blasting may have an adverse effect on nearby buildings or facilities that need to be protected, such as highwalls of open pit mines. For this reason, it is essential to make an acceptably accurate prediction of the vibrations, and therefore, define a safe charge of explosives

during blasting [12]. With the development of machine learning, an artificial neural network (ANN) method has increasingly been used in PPV prediction in recent years, it is becoming very easy to monitor and predict blast induced ground vibration [13].

Cognizant of the adverse effects of blast induced ground vibration it is therefore very essential to develop some prediction models and find ways of reducing the effects of ground vibration. The following are the empirical vibration predictor formulas developed by ancient researchers [14][15][16][17][18].

2.3 Air Blast

A blast of air pressure caused by the explosion of explosives is known as air-overpressure or airblast. Airblast is typically associated with frequency levels lower than 20 Hz, which is the threshold for hearing, and is generated by inadequate containment of the blast holes. Contrary to ground vibration, air blast rarely damages structures, but because of its loudness, it greatly annoys and disturbs nearby residents. These typically spark protests and turmoil in the local communities, as well as legal action from the impacted areas. Maximum charge per delay, distance from transducer, weight and spacing, stemming, direction of commencement, and charged depth are all factors that directly affect airblast. Additionally, other factors including weather, overcharging, weak strata, and secondary blasting conditions can also have an impact [19]. When the monitoring device is sensitive to low frequencies, as in [19], the research indicates that monitored air blast amplitudes of up to 135 dB are safe for structures (down to 1 Hz). Basic precautions should be taken, though, to limit the airblast levels produced by blasting operations below 115 dBL in crucial areas where the public is at risk [20]. Reference [20] has published the following estimates of damage thresholds based on empirical data.

Airblast is caused by the following reasons:

1. Direct rock displacement at the blast bench during the course of the blast that is the Air Pressure Pulse (APP),
2. Induced by ground vibration at some distance away from the blast that is the Rock Pressure Pulse (RPP),
3. Venting of blast holes or blowouts of gases through rock fractures that is the Gas Release Pulse (GRP).
4. Escape of gases from the blasthole when the stemming is ejected that is Stemming Release Pulse (SRP).

Air Pressure Pulses (APP) and Rock Pressure Pulses (RPP) are inescapable sources of airblast in bench blasting. Gas release pulses and stream release pulses, however, can be prevented through blast design [21]. Stemming release pulse and gas release pulse depend upon spacing, stemming, detonation velocity and burden. S.R.P. and G.R.P. appear as series of spikes which are combined on the APP. The acceptable limit for air blast which is currently recommended is 115 dB and anything above that is hazardous. This is concerned very much about welfare of the public and the environment. Air-overpressure is pressure acting and should not be confused with sound that is within audible range (detected by the human ear). [21].

Reference [22] researchers contacted an investigation on the influence and impact of simultaneous airblast forces and

ground shock on general structures and found out that, airblast load controls the structural damage and response in a relatively small scaled distance. Reference [23] researchers used site-specific Scaled Distances (SD) instead of conservative SD values to generate environmentally friendly and technically practicable results.

2.4 Artificial Neural Network (ANN)

The word artificial in neural networks indicates that it is not natural but Artificial Neural Network is inspired by the human brain. The original neural network refers to the human biological neural network which means the human brain and also brings out the focus of the artificial neural network which is to function like a human brain. The billions of nerve cells or neurons in the human brain have over a trillion connections between them. There are trillions of connections between these billions of neurons to allow information to flow from one neuron to another, transforming the human brain into an incredibly large network of interconnected neurons that can perform a variety of tasks, including, forecasting, decision-making and recognition, in a remarkably short period of time [24]. This inspired the researchers to look for the ways in which a computer can be made to imitate the large amounts of interconnection and networking which exist between all the nerve cells and the answer therefore becomes deep learning and machine leaning. The learning and training processes of the artificial neural networks can also be utilized to carry out these activities, turning them into a type of computing system that is intended to mimic how the human brain analyzes and processes information.

However, in engineering applications, only one task can typically be carried out at a time. Fortunately, the use of ANN for various engineering applications speeds up the process performances. In real life, the human brain performs multiple tasks in parallel. The human brain constantly performs multi-directional and decision-based tasks, but artificial neural network technologies are not trained to produce biological machines; instead, they are very close replicas of a very tiny portion of the original brain when doing certain tasks.

3. METHODOLOGY

The Rock Quality Designations (RQD) were obtained from the geological data, and some past blasting records were investigated to obtain the input and output data for the Artificial Neural Network operations. To obtain the optimum results nine interrelated input parameters were used and three outputs were obtained. The input parameters were burden, spacing, hole diameter, hole depth, distance from the blast site to the monitoring point, stemming length, maximum charge per delay, powder factor, and RQD. The output parameters were flyrocks, ground vibration and airblast. To create the optimum model, an ANN training is performed using inputs and outputs that are fed into the MATLAB-based ANN system. The produced ideal ANN model is then used in a number of blasts to achieve ideal outcomes by minimizing flyrock distances, ground vibration, and airblast.

To come up with the best ANN model to predict the required blasting parameters, the following steps shown in Figure 1 were used.

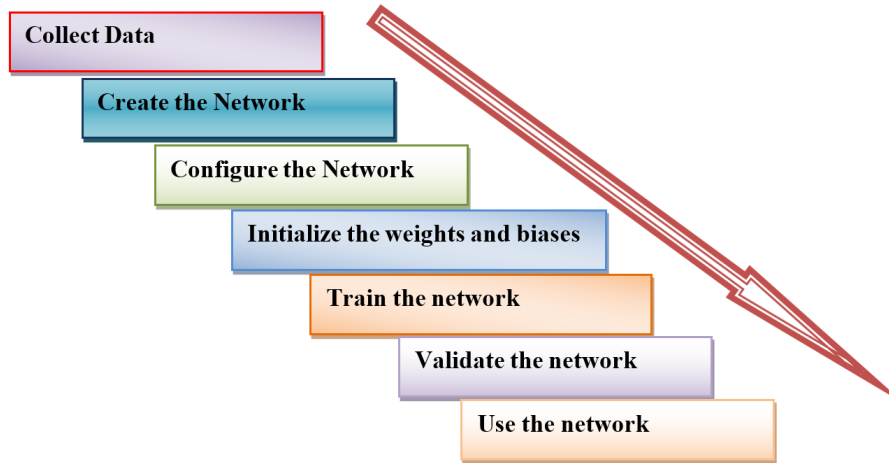


Fig. 1. ANN Methodology Flowchart

3.1 Data Collection

After blasting a flyrock analysis was carried out. The flyrock distances from the blast site were measured and the approximate amounts of flyrocks were recorded per each distance. On the basis of the rock type, blast hole depth and diameter, stemming length, charge delay, and powder factor, this data was then obtained for additional analysis and examination. An adaptable device known as the Instantel Micromate, which is equipped with a geophone and a microphone, was used to capture blast-induced ground vibrations and airblasts or air-overpressure. The devices measured the ground vibrations and airblasts at various

distances from the blast front, ranging from 42 m to 750 m. This includes all conceivably impacted locations, such as mining offices, processing facilities, engineering workshops, and worker housing.

3.1.1 Field Setup

Blasting seismographs are equipped to monitor ground vibrations and air overpressure, ground vibrations are set on three component direction and air overpressure are measured as a pressure wave. The seismograph stores the data digitally during an event. Annexure A and B shows data obtained from the seismograph during recording. Seismograph (number 11087) was used to monitor the airblast and ground vibration.

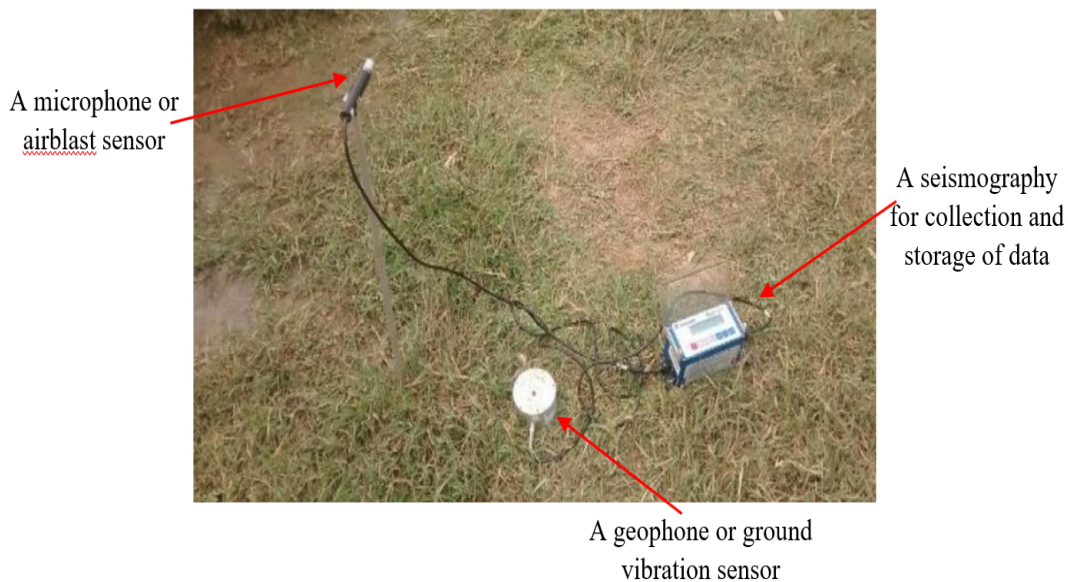


Fig. 2. Micromate field setup

A seismograph comprises of a geophone which is anchored into the ground and orientated to the blast, to register the ground vibration and an air pressure sensor which is placed at a height of between 0.3 – 1 m from the ground in order to register airblast. (This resembles a microphone.) The equipment activated on pre-set trigger levels on both ground vibration and

airblast figure 2. Set-up of the instruments which includes times when the instrument is active, with pre-set trigger levels for ground vibration and air blast. Trigger levels are the pre-programmed thresholds that cause the system to begin recording any event that exceeds those levels. Typically, the mechanism is activated by an air blast or ground vibration. The

thresholds that have been established assure accurate and efficient monitoring of every blast-related event while also reducing the likelihood of false triggers brought on by noise and vibration created in the area around the monitor.

The mine survey department provided the Geographical Positioning System (GPS) that was used to obtain the GPS coordinates of the blast and the location of the seismograph. The seismograph was placed at distances from 42 - 750m from the bench for each blast. The general wind direction was low with no cloud cover for most of the days when monitoring took place.

3.1.2 Input and Output datasets

A database of 100 blast data sets from various locations was taken in order to conduct the ANN analysis. The following variables were employed as inputs for the neural network modeling: hole depth, spacing, hole diameter, burden, stemming length, monitoring distance from the blast site, powder factor, maximum charge per delay, and Rock Quality Designation (RQD). All these input variable parameters, were chosen inputs because they significantly influence the flyrocks, ground vibration and airblast. However, some other variable parameters of low influence, significance and variation such as specific gravity of the rock have not been considered in the analysis. Thus, the analysis was carried out with nine input variables and their three corresponding output variables for 100 different blast data sets. These input variables and output variables have been represented in the table 1 and table 2 respectively.

Table 1. Input parameter ranges

Input Parameter	Symbol	Range
Spacing (m)	A	3.0 – 12.0
Burden (m)	B	2.0 – 12.00
Hole depth (m)	C	2.5 – 40.45
Hole diameter (mm)	D	130 - 310
Stemming length (m)	E	1.80 – 10.80
Powder factor (m ³ /kg)	F	1.52 – 2.02
Maximum charge per delay	G	28 – 1903.75
Rock Quality Designation	H	13 – 95
Distance from blast point to designation point (m)	I	42 - 750

Table 2. Output parameter ranges

Output Parameter	Symbol	Range
Flyrock (m)	M	23 – 56
Ground vibration / PPV (mm/s)	N	1 – 18
Airblast (dBL)	O	130 – 178

3.2 ANN Network Architecture

The phrase "Feed-forward back-propagation" refers to a forward flow activation of inputs and the backward error propagation of the weight adjustment to yield the actual output. All the output-related parameters must be involved and sent to the network as inputs in order to carry out a reliable mapping [25].

The Feed-forward Back-Propagation Neural Network (FBPNN) is developed using an input-output prediction modelling in form of a three layer which is defined by an input layer, a hidden layer and an output layer [26][27]. The ANN architecture used in this analysis has been shown in Figure 3. This FBPNN is used to forecast airblast, flyrocks, and ground vibration caused by blasts. It is more advantageous since it can handle a lot of data, it can handle situations that are quite complicated, and it works well for non-linear fits. Between some input patterns and some target patterns, it offers an acceptable mapping.

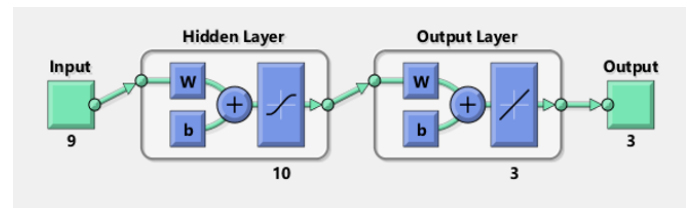


Fig. 3. ANN Architecture

The Bayesian Regularization training algorithm was chosen because, despite requiring more time, it produces high generalization for challenging, tiny, and noisy datasets. The training always stops according to the adaptive weight minimization (regularization). The linear combination of squared errors and weights is consistently minimized via Bayesian regularization. Additionally, it changes the linear combination so that the final network has high generalization capability [28][29][30]. In order to build the network, the performance factors such as the Mean square error (MSE), the number of layers, the number of neurons, and the transfer function are all chosen appropriately. After the network has been effectively created, it must then be trained. The study utilized a total of 100 data sets where 80% of the entire data was used for training, 10% for testing, and 10% for data validation.

3.3 Multivariate Regression Analysis (MVRA)

To forecast the linear relationship between the dependent variable and the independent variable(s), multivariate regression analysis is utilized. It makes use of the maximization principle, which seeks to minimize the sum of squares between the anticipated and measured values. It is described as in (1).

$$Y_i = \beta_0 + \beta_1 X_{i1} + \beta_2 X_{i2} + \beta_3 X_{i3} + \beta_4 X_{i4} + \dots + \beta_k X_{ik} \tag{1}$$

Where: Y_i is the predicted output,

β_0 is the intercept value,

$\beta_1, \beta_2, \beta_3, \beta_k$ are the regression coefficients,

$X_{i1}, X_{i2}, X_{i3}, X_{ik}$ are independent variables.

Using the coefficient of determination (R^2), the predictive power of the MVRA equation is assessed [31]. The MVRA prediction model's accuracy rises as R^2 approaches one and declines as R^2 moves inexorably in the direction of zero.

The derived MVRA model for flyrock prediction in this research is shown in (2):

$$\text{Flyrock (m)} = [[15.90419 + [0.564372 \times \text{Burden}] + [0.489943 \times \text{Spacing}] + [0.016448 \times \text{Hole diameter}] + [-0.38841 \times \text{Hole depth}] + [0.135902 \times \text{Stemming length}] + [-0.93878 \times \text{Powder factor}] + [0.007085 \times \text{Maximum Charge per delay}] + [-0.00063 \times \text{RQD}] + [-0.00244 \times \text{Monitoring distance}]] \quad (2)$$

The derived MVRA model for ground vibration has been shown in (3):

$$\text{Ground Vibration (PPV in mm/s)} = [[-4.813514 + [-0.764625 \times \text{Burden}] + [-0.138656 \times \text{Spacing}] + [0.070961 \times \text{Hole diameter}] + [-0.053073 \times \text{Hole depth}] + [0.752193 \times \text{Stemming length}] + [3.542046 \times \text{Powder factor}] + [-0.004284 \times \text{Maximum Charge per delay}] + [-0.026798 \times \text{RQD}] + [-0.029736 \times \text{Monitoring distance}]] \quad (3)$$

4. RESULTS AND ANALYSIS

The Flyrocks, ground vibration, and airblast were predicted using artificial neural networks and multi-variate regression analysis. The prediction performance of the ANN and the MVRA models was compared using the Root Mean Square Error (RMSE) and the Coefficient of Determination (R²). Both the ANN and the MVRA models' indexes for the various output parameters were computed.

4.1 ANN Model Performance.

The Neural network was trained and took 195 epochs to learn the data as shown in Figure 4.

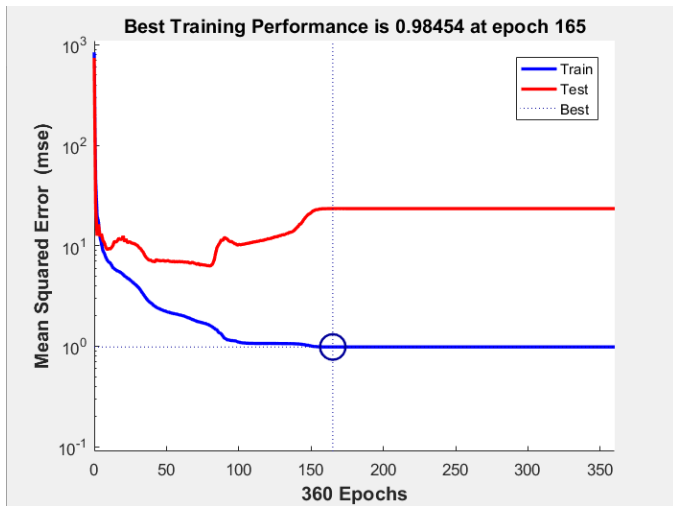


Fig. 4. ANN training graph

The performance of the model was evaluated by comparing the predicted and the measured values of the flyrocks, ground vibration and airblast. A graphical comparison of the predicted and the measured values is shown in the following Figures 5-10. A close analysis of these figures shows a very high correlation and conformity between the measured and the predicted values for each and every blasting pattern.

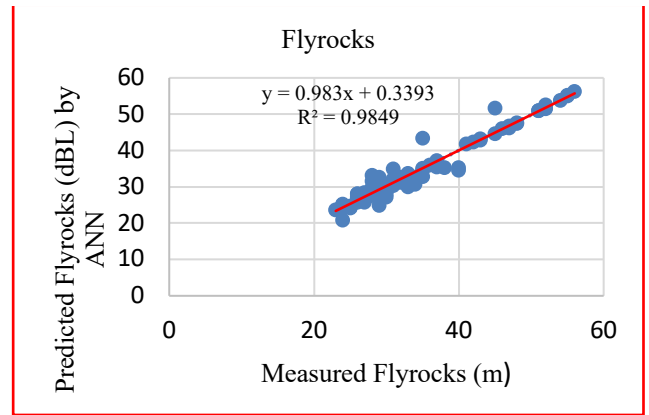


Fig. 5. Relationship between flyrocks measured values and predicted values by ANN

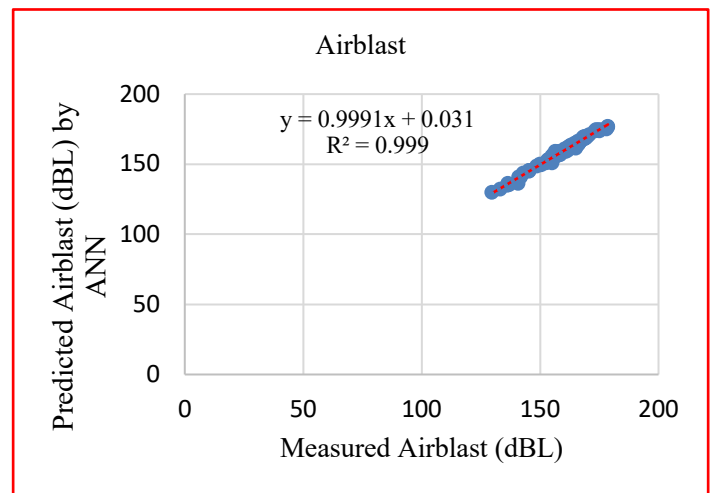


Fig. 6. Relationship between Airblast measured values and predicted values by ANN

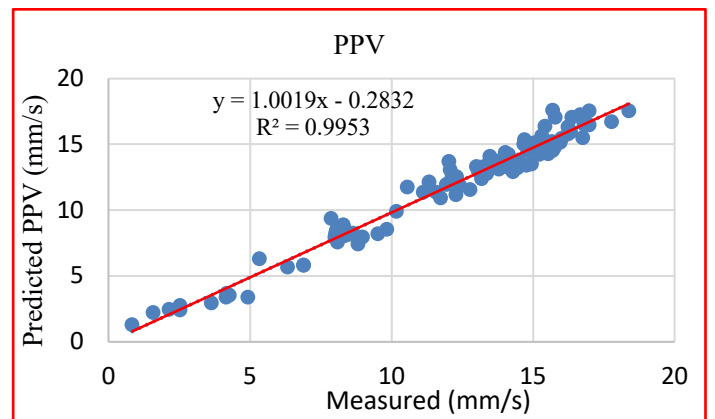


Fig. 7. Relationship between PPV measured values and predicted values by ANN

4.2 MVRA Model Performance.

Prediction values were generated and used to find the relationship between the measured values and the values predicted by the MVRA. The relationship graphs were presented as follows.

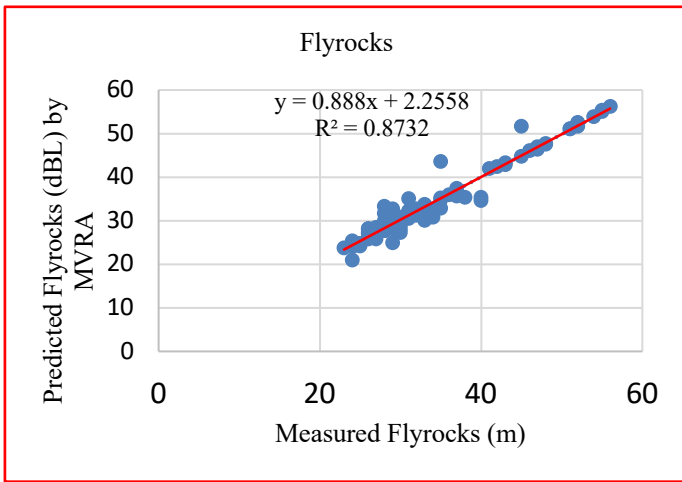


Fig. 8. Relationship between Flyrock measured and predicted values by MVRA

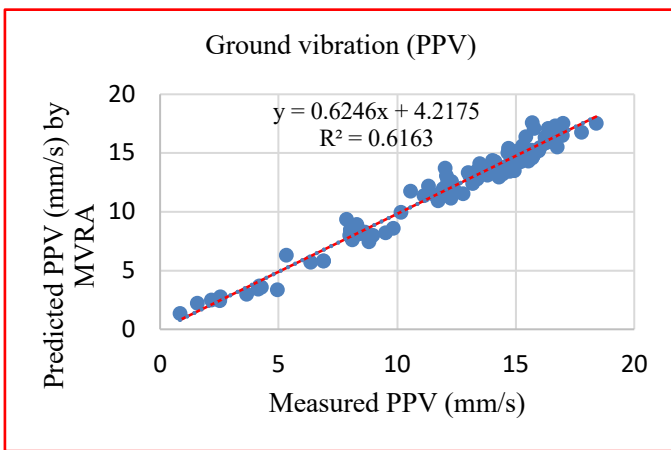


Fig. 9. Relationship between PPV measured and predicted values by MVRA.

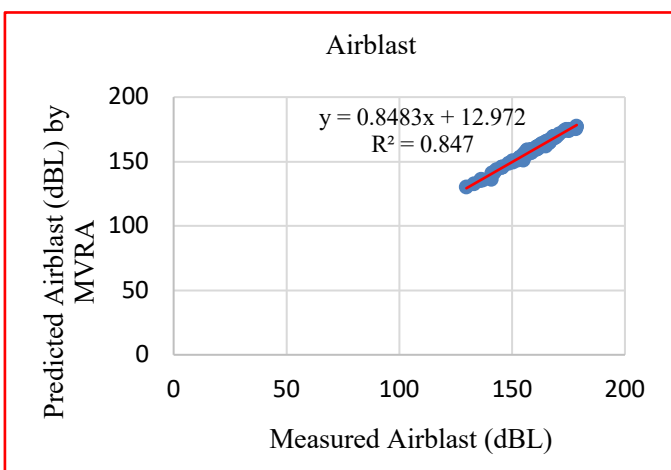


Fig. 10. Relationship between Airblast measured and predicted values by MVRA

4.3 Analysis of ANN and MVRA Model Performance.

The accuracy comparison between the ANN prediction and the MVRA prediction was basing on the value of R². It has been noted that the value of R² in ANN prediction is greater than that

of MVRA in all the three predictions (Flyrock, Ground vibration and Airblast analyses) which means that the ANN prediction proved to be more accurate than the MVRA prediction.

4.4 Sensitivity Analysis.

It examines how changes in certain parameters impact the behavior of the output of the model. It is done to increase reliability and robustness of a model by identifying the parameters which greatly affect the output behavior. It can also be used to reduce costs and improve performance by selecting the best and actual parameters which may have impact to the behavior of the model. Now to perform the sensitivity analysis, all data pairs were used for building a data array X as follows:

$$X = \{ x_1; x_2; x_3; \dots; x_i; \dots; x_n \} \tag{4}$$

The variable xi in the data array X is a length vector of m as:

$$X_i = \{ x_{i1}, x_{i2}, x_{i3}, \dots, x_{im} \} \tag{5}$$

The equation as follows presents the strength of the relation (r_{ij}) between the dataset X_i and X:

$$r_{ij} = \frac{\sum_{k=1}^m x_{ik}x_{kj}}{\sqrt{(\sum_{k=1}^m x_{ik}^2 \sum_{k=1}^m x_{kj}^2)}} \tag{6}$$

Where: r_{ij} = sensitivity strength, x_{ik} = inputs, x_{ij} = outputs

After computations of some strength figures, the data is then presented graphically to establish the strengths of the relations (r_{ij}) between the model inputs and output. The larger the R_{ij} is, the higher the influence of relevant input. The higher the influence of the input parameter to the output, the closer the R_{ij} to one. The results are shown graphically in Figures 11 - 13.

Key

- 1 - Burden, 2 -Spacing, 3 -Hole diameter, 4 - Hole Depth,
- 5 - Stemming, 6 - Powder Factor, 7 - Max Charge/delay,
- 8 - RQD, 9 - Monitoring Distance

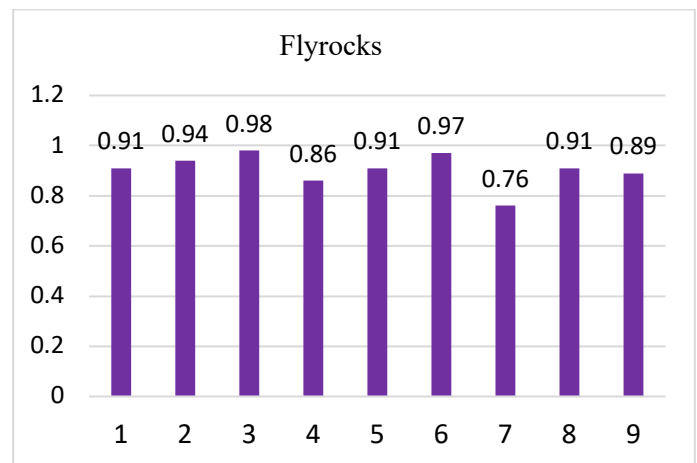


Fig. 11. Flyrock sensitivity analysis of inputs

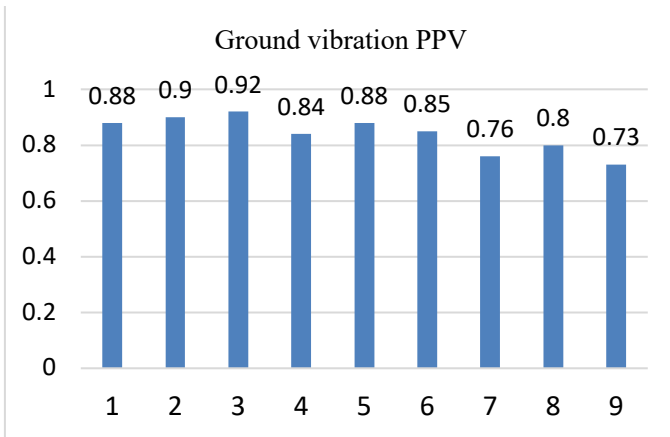


Fig. 12. Ground vibration sensitivity analysis with inputs

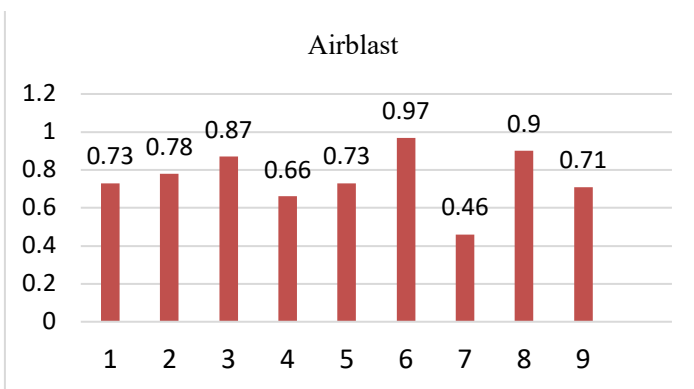


Fig. 13. Airblast sensitivity analysis of inputs.

Figure 11 and 12 illustrates that the most influential parameter for flyrocks and ground vibration is the hole diameter and on airblast, figure 13 demonstrates that the most influential is powder factor. Then the least on flyrocks and airblast is maximum charge per delay and on ground vibration is monitoring distance.

4.5 Root Mean Square Error (RMSE)

It is a method of evaluating how "well" the model fits a specific dataset. A regression model, an ANN model, or any other model that generates predicted values can be evaluated for how well it "fits" a dataset using the RMSE metric.

RMSE, is calculated as follows:

$$RMSE = \sqrt{[\sum(P_i - O_i)^2 / n]} \tag{7}$$

where:

P_i = the value predicted for the i^{th} observation in the dataset;

O_i = the value observed for the i^{th} observation in the dataset;

n = is the sample size.

The discrepancy between the predicted and observed values increases with RMSE, which also indicates how well the regression model fits the data. On the other hand, the better a model matches the data, the smaller the RMSE. Armstrong, J. Scott; Collopy, Fred (1992).

Table 3. Computed R^2 and RMSE for the comparison of ANN and MVRA

Model	Parameter	R^2	RMSE
ANN	Flyrocks	0.9849	0.047371
	Ground vibration	0.9953	0.078288
	Airblast	0.999	0.02402
MVR	Flyrocks	0.8732	0.16862
	Ground vibration	0.6163	1.302224
	Airblast	0.847	0.563716

Table 3 findings show that for all three forecasts, the ANN prediction's R^2 value is higher than the MVRA prediction's, indicating that the ANN prediction is more accurate than the MVRA prediction. Additionally, in all three forecasts, the RMSE for the ANN prediction is lower than for the MVRA prediction, further indicating that the ANN prediction is more accurate than the MVRA prediction.

4.6 Blast Optimization using ANN

The optimum ANN model developed for the sake of improving the quality and efficiency of the blasting operations. The optimization was used to optimize eight (8) experimental blasts at ZCDC mine and the results were used to compare with eight (8) non-optimized blasts. The optimization was carried out considering the variations of mechanical and geotechnical properties as the study demonstrated that rock mass behaviours differ with the difference in mechanical and geotechnical properties. An increase in stemming length was done on rock masses with poor RQDs for example on holes of diameter 152 mm with a hole depth of 8 m, the stemming lengths was put at 3.8 to 4.6 m in order maximize the usage of explosive energy on rock fragmentation and reducing the powder factor as the rock mass was already weak and easier to break. The blast outputs without ANN application were presented in the table 4.

Table 4. Optimised and non – optimised blast results

Non-optimized blasts			Optimized blasts		
Flyrock (m)	PPVs (mm/s)	Air blast (dBL)	Flyrock (m)	PPV (mm/s)	Air blast (dBL)
42	7.77447	130.64	27	3.04084	115.07
35	6.67155	128.51	25	3.81376	119.45
47	5.42777	139.79	24	4.09774	116.33
50	9.99313	139.10	26	2.18716	114.62
39	6.38564	127.86	23	1.48125	119.07
35	10.7026	137.15	25	5.29112	114.85
40	9.82735	128.13	30	3.15201	117.32
42	11.9796	141.64	28	7.79642	121.30

The results of non-optimized blasts demonstrated that the PPVs and Airblasts recorded had been above the company set limits of 9.5 mm/s and 115 dBL respectively and also most rock fragments were outside the desired range with some exceeding 20 m from the blast area. It is unlikely that these results will

cause damage and however the blast design and optimization was key to prevent possible community complaints in the future. Whilst on the other hand, the results of the optimized blasts presented demonstrated a significant improvement following the simulation of the input blast parameters using the optimum ANN model before the blasting. The ground vibrations PPVs and Airblasts had been within the range of acceptable company limits. The rock fragmentation was also assessed and found within the acceptable range that can be handled easily by the loading and hauling equipment with most of them ranging from 40 cm diameter to 85 cm. These improvements were found very pertinent as they contribute most to the economics of the company. It can be appreciated that the quantity of explosive charge calculated to control flyrocks is proportional to the mass of fragments to be broken and thrown therefore the larger the powder factor the higher the chances of flyrocks as flyrocks are mostly caused by the improper distribution of confinement of the explosive charge, explosive energy, and mechanical strength of the rock. However, specific charge expressed as kg/m^3 of explosive is not a useful design parameter for rock throw as flyrocks usually originate from the bench top, highwall face, and the toe. The reason for this is that the throw velocity and lateral displacement of rock are related largely to the weight of rock blasted rather than to the volume.

The input parameters with the least PPV were studied and qualified as the optimum parameters for trial blasts. The highest ground vibration levels were recorded in rock formations with high RQDs and also those with larger hole diameter. In rock formations with low RQDs the PPV power was absorbed by discontinuities and hence decreased with distance.

The optimised / non optimized data demonstrate that most of the blasts contacted were within the mine's proposed airblast overpressure limit of 115 dBL, blasting can be successfully implemented using the prescribed blast parameters and initiation systems and decking the face row. It is suggested that the blasting parameters with larger blasthole diameters of about 310 mm produces larger amounts of Airblast. The airblast analysis has determined that a maximum of an 115 mm blast hole diameter should be utilized, and therefore the 115 mm blast hole diameter should be used, as the analysis indicates that the most blasting activities with larger parameters will be more sensitive to airblast overpressure compliance. Analysis of results also demonstrate that airblast varies with the different in lithology but to ensure airblast control in various lithologies. A minimum face, burdens and stemming length must be adhered to and to ensure that the minimum face burdens are not compromised, the blasts should be surveyed and the blast holes bore tracked and come up with a suitable blasthole layout. Surveying of blasts would also be required to determine accurate distances for developing a site airblast prediction equation, for better guidance in future blasts.

5. CONCLUSIONS

The study's major goal was to improve the blast quality and enhance the outcomes by reducing the adverse effects of blasting, such as flyrocks, ground vibration, and airblast, as well as safeguarding the environment around the blasting zone. To find the best model suitable for predicting blast effects, the ANN prediction model was utilized, followed by a comparison of the outcomes with those of MVRA. All blasting parameters

and tests were taken and done at Zimbabwe Consolidated Diamond Company. About 8 experimental blasts were optimized using the produced ANN model, and the outcomes were contrasted with those of 8 more unoptimized blasts. Both blast impacts and flyrock ranges were reduced using the ANN model. The study's findings were distilled into the following points:

1. The Bayesian Regularization training approach was used to create the best ANN model, which had a network design of 9-10-3, or (9 input parameters, 10 hidden neurons, and 3 output parameters). It has been determined that the coefficient of determination (R^2) is 0.9983.
2. The optimal ANN model has increased the blast efficiency by minimizing the ground vibration and airblast values below the specified corporate limitations of 20 meters, 9.5 millimeters per second, and 115 decibels, respectively.
3. The ANN model displayed an excellent and significant conformity between the measured values and predicted output values as compared to the MVRA model through the comparison of the R^2 and RMSE.
4. The sensitivity analysis has determined that the spacing, burden, stemming length, powder factor and hole diameter are the most effective and influential parameters on all the three outputs.

REFERENCES

- [1] R. K. Wharton, S. A. Formby, and R. Merrifield, "Airblast TNT equivalence for a range of commercial blasting explosives," *J Hazard Mater*, vol. A79, pp.31–9, 2000.
- [2] H. C. Verakis and T. E. Lobb, "An analysis of blasting accidents in mining operations," 29th Annual Conference on Explosives and Blasting Techniques, vol. 2, pp. 119-129. Cleveland: OH: International Society of Explosives Engineers. February 2003.
- [3] R. Trivedi, and T. Singh, A. Raina, "Prediction of blast-induced flyrock in Indian limestone mines using neural networks," *J. Rock Mech. Geotech. Eng.*, vol. 6, pp. 447–454, 2014.
- [4] M. Monjezi, H. Dehghan, and N. F. Samimi, "Application of TOPSIS method in controlling fly rock in blasting operations," *Proceedings of the seventh international science conference SGEM. Sofia Bulgaria, 2007.* pp. 41–49.
- [5] A. S. Tawadrous, "Evaluation of artificial neural networks as a reliable tool in blast design," *Int Soc Explos Engg.* vol. 1, pp.1–12, 2006.
- [6] A. Richards, A. Moore, A. "Flyrock control-by chance or design. In *Proceedings of the Annual Conference on Explosives and Blasting Technique*," New Orleans, LA, USA, 1–4, vol. 1, pp. 335–348, February 2004.
- [7] A. K. Raina, V.M.S.R. Murthy, A. K. Soni, "Flyrock in bench blasting: A comprehensive review," *Bull. Int. Assoc. Eng. Geol.*, vol. 73, pp. 1199–1209, 2014.
- [8] A. Robert, "Ground Vibration due to quarry blasting and other sources-An environmental factor in Rock mechanics," 12th Proc. symo. on Rock mechanics. New York: University of Missouri, AIME. pp. 427-456, 1971.
- [9] N.M. Djordjevic, "A Study on the Blast Induced Ground Vibrations and their Effects on Structures," PhD Thesis, Julius Kruttschnitt Mineral Research Centre, The University of Queensland, Brisbane, Australia, 1995.
- [10] M. Khandelwal, and T.N. Singh, "Evaluation of blast-induced ground vibration predictors," *Soil Dynam Earth Engg.*, vol. 27, pp. 116–25. 2007.
- [11] M. Hasanipanah, R. S. Faradonbeh, H. B. Amnieh, D. J. Armaghani, M. Monjezi, "Forecasting blast-induced ground vibration developing a CART model," *Eng. Comput.*, vol. 33, pp. 307–316, 2017.
- [12] H. R. Nichols, C. F. Johnson, W. I. Duvall, *Blasting vibrations and their effects on the structures.* USBM, Bulletin No. 656, pp. 105, 1971.

- [13] H. B. Amnieh, M. R. Mozdianfard, and A. Siamaki, "Predicting of blasting vibrations in Sarcheshmeh copper mine by neural network," *Safety Science*, vol. 48. pp. 319–325, 2010.
- [14] W. I. Duvall and D. E. Fogelson, "Review of criteria for estimating damage to residences from blasting vibrations," College Park, MD USA, Bureau of Mines, 1962.
- [15] U. Langefors and B. Kihlstrom, "The Modern Technique of Rock Blasting," Stockholm: Almgvist A Wiksell, 1963.
- [16] M. T. Mohamed, "Artificial neural network for prediction and control of blasting vibrations in Assiut (Egypt) limestone quarry," *Int J Rock Mech Min Sci*, vol. 46, pp. 426–43. 2009.
- [17] A. Richards, "Elliptical airblast overpressure model," *Mining Technology*, ISSN 1474-9009, vol. 119, pp. 205-211. 2010.
- [18] T. M. Mostafa, "Artificial neural network for prediction and control of blasting vibrations in Assiut (Egypt) limestone quarry," *Int J Rock Mech Min Sci*, vol 46(2), pp. 426–431. 2009.
- [19] D. E. Siskind, M. S. Stagg, J. W. Kopp and D. Dowding, "Structural response and damage produced by ground vibration from Surface Mine Blasting," US Bureau of Mines RI8507, USA, 1980.
- [20] P. A. Perrson, "The relationship between strain energy, rock damage, fragmentation and throw in rock blasting," *Int. J. Blasting Fragmentation*, vol. 1, pp. 99 –109, 1997.
- [21] P. Segarra, "Prediction of near field overpressure from quarry blasting," *Applied Acoustics*, vol. 71(12), 1169-1176, 2010.
- [22] C. Wu, and H. Hao, "Modeling of simultaneous ground shock and airblast pressure on nearby structures from surface explosions," *International Journal of Impact Engineering*, ISSN 0734-743X, vol. 31(6), pp. 699-717, 2007.
- [23] R. Pal, "Rock blasting effects and operations," Rotterdam: Balkema, pp. 23–40, 2005.
- [24] M. Saadat, M. Khandelwal, and M. Mojezi, "An ANN-based approach to predict blast-induced ground vibration of Gol-E-Gohar iron ore mine," *Iran Journal of Rock Mechanics and Geotechnical Engineering*. Vol. 6(1), pp 67-76, 2014.
- [25] A. Bahrami, M. Monjezi, K. Goshtasbi, and A. Ghazvinian, "Prediction rock fragmentation due to blasting using artificial neural network. *Engineering with Computers*," vol 27(2), pp. 177–181, 2011.
- [26] J. Roman, and A. Jameel, "Backpropagation and recurrent neural networks in financial analysis of multiple stock market returns," *Proceedings of the Twenty-Ninth Hawaii International Conference on System Sciences*, vol. 2, pp. 454–460, 1996.
- [27] M. Hajihassani, D. J. Armaghani, H. Sohaei, E. T. Mohamad, and A. Marto, "Prediction of airblast-overpressure induced by blasting using a hybrid artificial neural network and particle swarm optimization," *Applied Acoustics*, vol. 80, pp. 57–67, 2014.
- [28] D. J. C. Mackay, "Bayesian interpolation," *Neural Computation*, vol 4(3), pp. 415–447, 1992.
- [29] M. Monjezi, T. N. Singh, M. Khandelwal, S. Sinha, V. Singh, and I. Hosseini, "Prediction and analysis of blast parameters using artificial neural network," *Noise Vibrat Worldwide*, vol. 37, pp. 8–16. 2006.
- [30] A. M. Remennikov, and P. A. Mendis, "Prediction of airblast loads in complex environments using artificial neural networks," *WIT Trans on the Built Environ*, vol. 87, pp. 269–278, 2006.
- [31] I. Enayatollahi, B. Aghajani, A. Abbas; A. Ahamad, "Comparison between Neural Networks and Multiple Regression Analysis to Predict Rock Fragmentation in Open-Pit Mines," *Rock Mechanics and Rock Engineering*, vol. 47(2), pp. 799–807, 2014.